JOURNAL OF Materials CHEMISTRY

Photocatalytic and photoelectrochemical properties of TiO_2-based multiple layer thin film prepared by sol–gel and reactive-sputtering methods

Atsuo Yasumori,* Hiroyuki Shinoda, Yoshikazu Kameshima, Shigeo Hayashi and Kiyoshi Okada

Department of Metallurgy and Ceramic Science, Tokyo Institute of Technology, Tokyo, 152-8552, Japan. E-mail: ayasumor@ceram.titech.ac.jp

Received 4th January 2001, Accepted 23rd January 2001
First published as an Advance Article on the web 2nd March 2001

The multiple layers of a TiO_2 thin film, consisting of a TiO_2 thin film, a platinum electrode and a porous alumina substrate, were prepared by the sol–gel method in a previous study. As a sputtering process has some advantages over wet-chemical processes, especially for practical manufacturing, a thin film photocatalyst with the same layer structure was prepared by the reactive-sputtering method in this study. The TiO_2 thin film of the photoactive anatase phase was formed by using an appropriate gas pressure and temperature, however, the crystallite size of anatase was almost twice as large and the band gap energy was slightly smaller than those of the sol–gel-processed thin film. The sputtering-processed thin film showed a typical columnar structure with some voids. The lower band gap energy and the coarse structure probably promoted the recombination between photoexcited electrons and holes, and resulted in lower photocatalytic activity and photocurrent compared with the sol–gel-processed thin film.

To date, a considerable amount of work has been carried out using metal oxide semiconductor photocatalysts for the purposes of solving various environmental issues. The form of the TiO_2 photocatalyst seems to shift from a particulate into a thin film, providing the large reaction surface area and easy handling characteristics which are necessary for the pratical application of photocatalytic materials in areas such as: the photodecomposition of chemical pollutants in water and atmospheric purification,[1–3] and anti-dirtying and anti-fogging coatings.[4,5]

Most TiO_2 thin film photocatalysts are prepared using wet-chemical processes such as the sol–gel method, mainly due to the advantages of simple equipment requirements, low cost and the ease with which large or complicated surfaces can be coated. In our previous study, a multiple layer photocatalyst comprising a TiO_2 thin film and a platinum electrode was fabricated on a porous alumina substrate by use of the sol–gel method in order to reconcile the advantages of the fine particles with those of thin films.[6] This system showed high photocatalytic activity because it behaved like a "self-standing" nanometer thin film system which could spatially separate the oxidation and reduction sites and create short diffusion distances to the surface for the photogenerated charge carriers.

TiO_2 thin films prepared using sputtering methods are practically utilized as anti-reflective coatings for optical components and photonic devices.[7–9] The sputtering method has some advantages over wet-chemical processes, namely its simplicity (it is a one-step process) and the easy control of film thickness. Owing to these significant advantages, there has been a recent widespread interest in TiO_2 thin film photocatalysts prepared by the sputtering method.[10–14] However, no studies have been reported where the difference in photocatalytic activity between the sputtering- and sol–gel-processed thin films has been investigated.

In this study, the same multiple layer TiO_2 photocatalysts were fabricated by using the sol–gel (SG) and the reactive-sputtering (RSP) methods. The photocatalytic and photoelectrochemical properties of the prepared thin film systems were examined. The differences in photocatalytic activity and its origins are discussed based on the natures of the thin films.

Experimental

Sample preparation

A flowchart for the fabrication of the thin film photocatalyst is shown in Fig. 1. The TiO_2 thin film sample was prepared by the reactive-sputtering method (abbreviated as RSP) with RF magnetron sputtering (Nichidn-ANELVA, SPF-210H) on a porous alumina substrate covered with silica gel and platinum layers.[6] A titanium target (Furuuchi-kagaku, 99.9%) and Ar(90%)–O_2(10%) gas mixture were utilized as reaction sources. The pressure during sputtering was 3.5, 30, 60 or 90 mTorr (0.47, 4.0, 8.0, 12 Pa, respectively), and the substrate

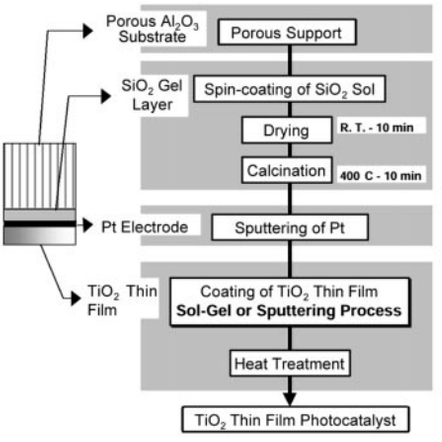

Fig. 1 Flowchart for the fabrication of the multiple layer TiO_2 thin film photocatalyst.

was kept under non-heated conditions or heated at either 200 or 100 °C.

Another sample (denoted SG) was prepared through the sol–gel method which we have already reported, that is, the porous substrate was coated with stabilized TiO_2 sol, and was finally heat-treated at 400 °C.[6] In both methods, glass substrates and platinum foils were also utilized as substrates for optical and electrochemical measurements of TiO_2 thin films.

Characterization

Crystalline phases of the samples were identified by X-ray diffraction (XRD) measurements. The surface and a cross-section of the sample were observed by scanning electron microscopy (SEM). The transmittance of the TiO_2 thin film coated on the glass substrate was measured using a UV-Visible spectrometer (JASCO V-570) for evaluation of the band gap energy and the thickness of the TiO_2 thin film. The surface roughness was measured on a roughness meter (Tokyo-Seimitsu, Surfcom 1400) and was used to give an indication of film thickness. The photocatalytic activity was evaluated by measuring the photogeneration rate of hydrogen from 20 vol% aqueous ethanol solution under an argon atmosphere. Details of the measurements are shown in the previous report.[6]

The photocurrent–potential curves of the samples were measured on a three electrode system combined with a potentiostat (Hokuto-Denko, HA-301) and a function generator (HP 165A). In this electrode system the working electrode was TiO_2 thin film coated on platinum foil, the counter electrode was a platinum wire and the reference electrode was a saturated calomel electrode (SCE). The buffered solution (acetic acid, sodium acetate, and potassium chloride in H_2O, pH = 4.60, under argon) was utilized during the measurements in order to prevent pH variation and to eliminate the effect of dissolved oxygen. IR spectra of the samples were measured on a FT-IR spectrometer (Shimadzu FTIR-8000PC) in order to evaluate the change in the surface structure of the TiO_2 thin film after the photochemical reaction.

Results

Crystalline phase and structure of the thin film

The XRD patterns of the RSP samples on various substrates are shown in Fig. 2 along with the pattern for the SG sample on a porous substrate. The TiO_2 crystalline phases of RSP samples under various conditions are listed in Table 1. Pressures higher than 30 mTorr resulted in the formation of an anatase phase, oriented along the (101) plane. As the temperature of the substrate increased, the degree of orientation decreased. The crystallinity of anatase became worse as the pressure increased.

The orientation of TiO_2 on the glass substrate was higher than that on the porous substrate with platinum, although there was not much difference in crystalline conditions for the substrates shown in Fig. 2. The strong orientation of platinum foil along the (220) plane (its diffraction peak, $2\theta = 67.5°$, is not shown in the figure) did not affect the orientation of TiO_2 thin film. There was no obvious difference between the RSP and SG samples except for the crystallinity.

The SEM images of the surfaces and cross-sections of (A) the SG sample (8 coatings, heat-treated at 400 °C) and (B) the RSP sample (gas pressure: 30 mTorr, no heat treatment, sputtering time: 4 h) are shown in Fig. 3. The secondary electron images (SEI) of the cross-sections show the pore structures of the porous alumina substrate and the upper-layers. In the back electron images (BEI), the bright line was identified as the platinum layer. The thickness of the TiO_2 layer on the substrate was estimated from the SEI + BEI images. The TiO_2 layer in the SG sample consisted of nanometer-size fine particles. The TiO_2 layer in the RSP sample showed the typical columnar structure

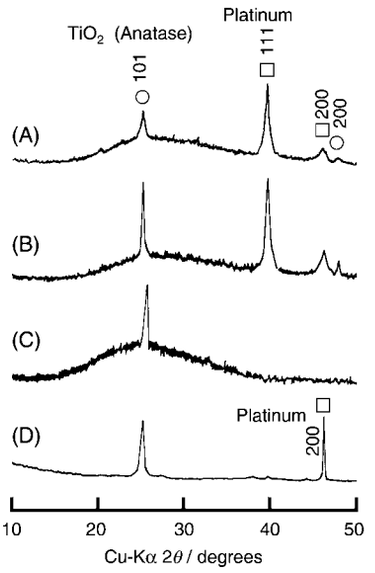

Fig. 2 XRD patterns of the TiO_2 thin films on various substrates: (A) Sol–gel-processed thin film on a porous substrate, (B) Sputtering-processed thin film on a porous substrate, (C) Sputtering-processed thin film on a glass substrate, (D) Sputtering-processed thin film on a platinum foil.

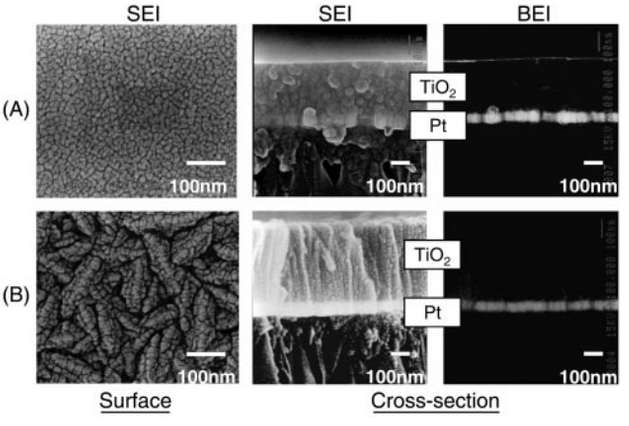

Fig. 3 SEM images of the surface and a cross-section of the multiple layer photocatalysts from: (A) The sol–gel process, (B) The sputtering process.

for materials prepared by the sputtering method. This difference in the structures reflected the difference in the surface morphologies of the thin films.

The transmittances of the samples were more than 80% in the visible range with peaks and valleys due to interference from the thin film. Absorption edges of the samples were at around 350 nm or less. The film thickness of 390 nm for the RSP sample (4 h sputtering), obtained by use of the peak–valley method, was intermediate between the value of 420 nm obtained from the SEM observations and 330 nm from the surface roughness measurement.

Photocatalytic and photoelectrochemical properties

The amounts of photogenerated hydrogen per unit surface area of the samples are shown in Fig. 4. The amount of hydrogen from the SG sample was over twenty times larger than that from the RSP sample, though the film thickness of the former, *ca.* 240 nm (8 coatings), was thinner than that of the latter, *ca.* 390 nm (4 h sputtering).

The photocurrent–potential curves of the SG and RSP

Table 1 Crystalline phase of the TiO_2 thin film obtained under various sputtering conditions[a]

Temperature	3.5 mTorr (0.47 Pa)	30 mTorr (4.0 Pa)	60 mTorr (8.0 Pa)	90 mTorr (12 Pa)
RT	R(GL)	A(GL)	—	—
	—	A(PT)	—	—
	—	A(PS)	A(PS)	A(PS)
100 °C		—		
		—		
		A(PS)		
200 °C	A + R(GL)	A(GL)		
	R(PT)	—		
	—	A + R(PS)		

[a]A: Anatase, R: rutile, GL: glass, PT: platinum foil, PS: porous substrate.

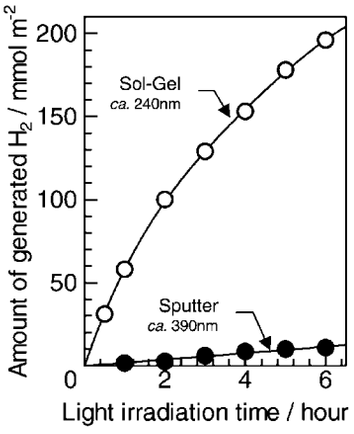

Fig. 4 Amounts of photogenerated hydrogen per unit surface area from the multiple layer TiO_2 thin film photocatalysts.

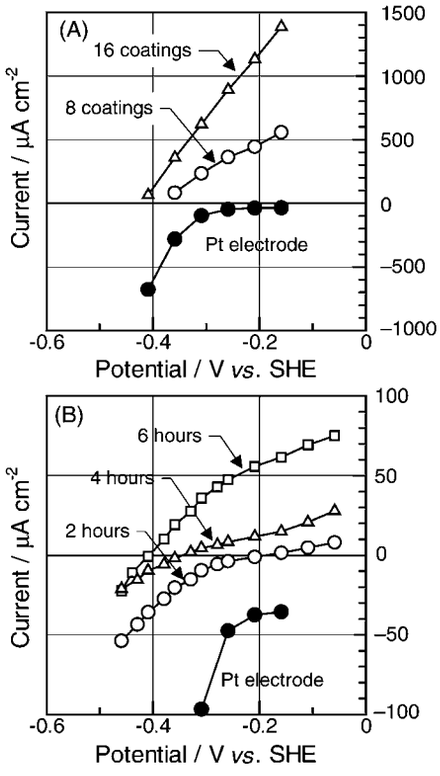

Fig. 5 Photocurrent–potential curves of the TiO_2 thin film electrodes: (A) Sol–gel process, (B) Sputtering process.

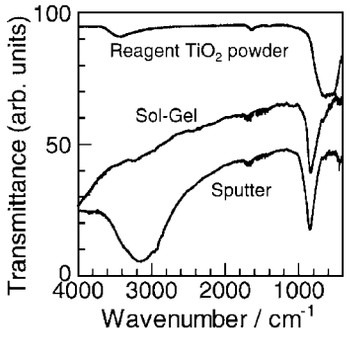

Fig. 6 IR spectra of the TiO_2 thin film electrodes and reagent grade TiO_2 powder.

electrodes in the buffered solution are shown in Fig. 5(A) and (B), respectively. The current of a single platinum electrode was measured instead of the dark current of the samples, because the coated TiO_2 thin films were prone to peeling off the platinum foil substrate, especially when the negative potential was applied to the samples under dark conditions. In the figures, the applied potentials *vs.* SCE in the experiments have been converted into applied potentials *vs.* a standard hydrogen electrode (SHE). In both processed samples, the photocurrent increased with film thickness. The flat-band potentials estimated from the current–potential curves were about −0.4 V *vs.* SHE for all the samples. The photocurrent of the SG sample was much larger than that of the RSP sample.

The diffuse reflectance IR spectra of the SG and RSP samples after photoelectrochemical measurements are shown in Fig. 6 with the transmittance spectrum (KBr method) of the reagent grade TiO_2 (anatase) powder. The spectrum of the SG sample has only a strong absorption peak for TiO_2 at around 900 cm^{-1}, though it has shifted to higher wavenumber than that of TiO_2 powder as a consequence of the particle size effect.[15] In addition to the peak at *ca.* 900 cm^{-1} the RSP sample has another large, broad peak at around 3000 cm^{-1}, which is due to Ti–OH groups.

Discussion

Morphology and crystallinity of the thin film

The sputtering conditions which mainly affected the crystalline phase of TiO_2 were the gas pressure and the temperature. The results suggested that lower gas pressures and higher temperatures led to the formation of a stable crystalline rutile phase. Meng and Dos Santos studied the effects of gas pressure and temperature on the structure of sputtering-processed thin films.[16] They reported that, in general, lower gas pressures and higher temperatures led to a dense thin film which consisted of a stable crystalline phase. Our results of a metastable crystalline phase (anatase) and the columnar coarse structure of the thin film at the higher gas pressure and lower temperature are therefore in good agreement with their conclusions. The structure and crystallinity of the SG sample were very different to those of the RSP sample. The SG sample showed a dense structure, crystallite sizes of anatase estimated by Scherrer's method were 29 nm in the RSP and 15 nm in the SG sample.

Optical band gap of the thin film

The above-mentioned difference in crystallite size resulted from the difference in the optical band gap energy of the TiO_2 thin films. The band gap energy can be estimated from the absorption edge of the UV-Visible spectrum by use of the following equation.[17]

$$\alpha \cdot h\nu = A(h\nu - E_g)^n$$

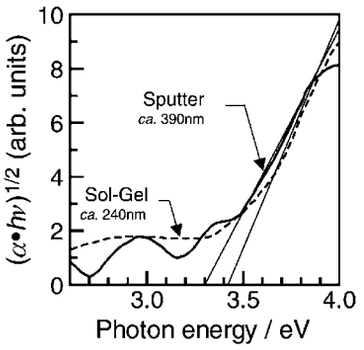

Fig. 7 Plots of $(\alpha \cdot h\nu)^{1/2}$ against $h\nu$ for the sputtering and the sol–gel-processed TiO_2 thin films.

Here, α is the absorption coefficient near the absorption edge, ν is the frequency, A is a constant, E_g is the band gap energy and n is a constant related to the type of optical transition. The light absorption of TiO_2 is caused by an indirect transition,[18] so that n is 2. Plots of $(\alpha \cdot h\nu)^{1/2}$ against $h\nu$ for the RSP and SG samples are shown in Fig. 7. The obtained band gap energies were 3.30 eV for the RSP and 3.42 eV for the SG sample. These values were slightly larger than that for the anatase single crystal: 3.2 eV.[19] The film thicknesses of the RSP and SG samples were *ca.* 390 nm and 240 nm, respectively, which were thick enough compared with crystallite sizes of 29 nm and 15 nm. These results indicate that the increase in the band gap energies and their difference between the two samples was caused by a change in band structure as a result of differing crystallite sizes.

Photocatalytic activity

In our multiple layer systems, the potential gradients of both the conduction and valence bands of TiO_2 were formed across the TiO_2 layer.[6] The photoexcited electrons diffused to the platinum electrode, and the holes ought to diffuse toward the surface of the TiO_2 thin film along the potential gradients. In the photocurrent–potential curves of both the RSP and the SG samples the flat band potentials were very similar. This suggests that the reducing ability of photoexcited electrons is almost the same in both samples. However, the photocurrent of the SG sample was 20–30 times larger than that of the RSP sample, coinciding with their photocatalytic activities.

The probable reactions which have an effect on photocatalytic activity and photocurrent in our system are (1) recombination between the photoexcited electrons and holes, and (2) reactions at the surface of TiO_2 between the holes and oxidation products which is the rate-determining step in photocatalytic redox reactions. In the former reactions, the larger band gap energy suppresses the direct recombination between the photoexcited electrons and holes. The band gap energy of the SG sample, 3.42 eV, was larger than that of the RSP sample, 3.30 eV, which is advantageous for the suppression of the recombination. Another property of the thin film which may affect the recombination is its defect structure because most recombination occurs indirectly at the lattice and surface defects of the TiO_2 layer. The thin film structure of the RSP sample was much coarser than that of the SG sample, suggesting that the former has more surface defects which may act as recombination centers, that is, the coarse structure of the RSP sample promotes the recombination. It is plausible that the separation of photoexcited electrons and holes proceeds much more efficiently in the dense film of the SG sample, as schematically illustrated in Fig. 8, and that this effective separation of charge carriers results in the much higher photocatalytic activity and photocurrent observed.

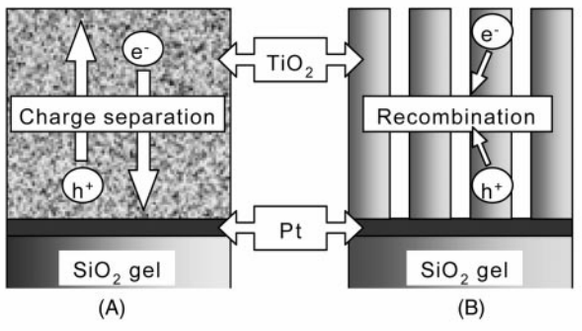

Fig. 8 Schematic illustrations of the TiO_2 thin film photocatalysts: (A) Sol–gel process, (B) Sputtering process.

In the latter surface reactions, the structural change of the TiO_2 layer due to the different processes would change the density of surface OH groups and surface lattice defects, which mainly consist of Ti^{3+} ions and oxygen vacancies.[20–22] In the IR examinations, the amount of OH groups in the RSP sample was larger than in the SG sample, clearly showing that the number of recombination sites was larger in the coarse structure of the RSP sample.

Conclusions

The TiO_2 thin film of the photoactive anatase phase was obtained by the reactive-sputtering method using the appropriate gas pressure and temperature. The sputtering-processed thin film showed a typical columnar structure with some voids. The lower band gap energy and the coarse structure promoted the recombination of photoexcited charge carriers, resulting in much lower photocatalytic activity compared to the sol–gel-processed sample.

It is clear that this arrangement of the TiO_2 thin film and the platinum electrode on a porous substrate makes a contribution to the high activity observed. In order to achieve the high photocatalytic activity of this multiple layer TiO_2 thin film system it was found that the dense TiO_2 thin film of the anatase phase must have a defect-free structure. The sol–gel method, which leads to less defects, is therefore superior to the sputtering process for the fabrication of such a system.

References

1 A. Fernández, G. Lassaletta, V. M. Jiménez, A. Justo, A. R. González-Elipe, J.-M. Herrmann, H. Tahiri and Y. Ait-Ichou, *Appl. Catal. B*, 1995, **7**, 49.
2 N. Negishi, T. Iyoda, K. Hashimoto and A. Fujishima, *Chem. Lett.*, 1995, 841.
3 I. Sopyan, S. Murasawa, K. Hashimoto and A. Fujishima, *Chem. Lett.*, 1994, 723.
4 Y. Paz, Z. Luo, L. Rabenberg and A. Heller, *J. Mater. Res.*, 1995, **10**, 2842.
5 T. Watanabe, A. Nakajima, R. Wang, M. Minabe, S. Koizumi, A. Fujishima and K. Hashimoto, *Thin Solid Films*, 1999, **351**, 260.
6 A. Yasumori, K. Ishizu, S. Hayashi and K. Okada, *J. Mater. Chem.*, 1998, **8**, 2521.
7 J. Szczyrbowski, G. Bräuer, G. Teschner and A. Zmelty, *J. Non-Cryst. Solids*, 1997, **218**, 25.
8 J. Szczyrbowski, G. Bräuer, G. Teschner and A. Zmelty, *Surf. Coat. Technol.*, 1998, **98**, 1460.
9 C. Battaglin, F. Caccavale, A. Menelle, M. Montecchi, E. Nichelatti, F. Nicoletti and P. Polato, *Thin Solid Films*, 1999, **351**, 176.
10 B. R. Weinberger and R. B. Garber, *Appl. Phys. Lett.*, 1995, **66**, 2409.
11 H. Wang, T. Wang and P. Xu, *J. Mater. Sci.*, 1998, **9**, 327.
12 J. Sheng, L. Shivalingappa, J. Karasawa and T. Fukami, *Vacuum*, 1998, **51**, 623.
13 N. Negishi, K. Takeuchi, T. Ibuski and A. K. Datye, *J. Mater. Sci. Lett.*, 1999, **18**, 515.
14 D. Dumitriu, A. R. Bally, C. Ballif, P. Hones, P. E. Schmid, R. Sanjinés, F. Lévy and V. I. Pârvulescu, *Appl. Catal. B*, 2000, **25**, 83.

15 R. Ruppin and R. Englman, *Rep. Prog. Phys.*, 1970, **33**, 149.
16 L.-J. Meng and M. P. Dos Santos, *Thin Solid Films*, 1993, **68**, 319.
17 H. Demiryont and J. R. Sites, *J. Vac. Sci. Technol. A*, 1984, **2**, 1457.
18 T. Yoko, A. Yuasa, K. Kamiya and S. Sakka, *J. Electrochem. Soc.*, 1991, **138**, 2308.
19 H. Tang, H. Berger, P. E. Schmid, F. Levy and G. Burri, *Solid State Commun.*, 1993, **87**, 847.
20 Y. Oosawa and M. Gratzel, *J. Chem. Soc., Faraday Trans. 1*, 1988, **84**, 197.
21 K. Kobayakawa, Y. Nakazawa, M. Ikeda, Y. Sato and A. Fujishima, *Ber. Bunsen-Ges. Phys. Chem.*, 1990, **94**, 1439.
22 A. Yasumori, K. Yamazaki, S. Shibata and M. Yamane, *J. Ceram. Soc. Jpn.*, 1994, **102**, 702.